Accepted Manuscript

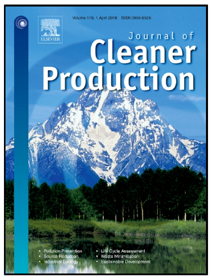

Development, Characterisation and Finite Element Modelling of Novel Waste Carpet Composites for Structural Applications

Adeayo Sotayo, Sarah Green, Geoffrey Turvey

PII:	S0959-6526(18)30407-4
DOI:	10.1016/j.jclepro.2018.02.095
Reference:	JCLP 12042
To appear in:	*Journal of Cleaner Production*
Received Date:	21 November 2017
Revised Date:	01 February 2018
Accepted Date:	09 February 2018

Please cite this article as: Adeayo Sotayo, Sarah Green, Geoffrey Turvey, Development, Characterisation and Finite Element Modelling of Novel Waste Carpet Composites for Structural Applications, *Journal of Cleaner Production* (2018), doi: 10.1016/j.jclepro.2018.02.095

Word count – 7060

Development, Characterisation and Finite Element Modelling of Novel Waste Carpet Composites for Structural Applications

Adeayo Sotayo*[a b], Sarah Green [a] and Geoffrey Turvey [a]

[a] **Engineering Department, Lancaster University, Bailrigg, Lancaster, LA1 4YR. UK**

[b] **School of Engineering, University of Liverpool, Liverpool, L69 3GH**

Abstract

Carpets are composite materials and, like many composite materials, waste carpet is both difficult and expensive to recycle because of the complicated, multi-stage processes involved. Consequently, in the United Kingdom, approximately 400,000 tonnes of carpet waste are sent to landfill annually. However, the landfill option is becoming uneconomic due to increasing landfill charges, the reduction in landfill sites and changes in environmental legislation. This dual economic and environmental burden has led to research interest in the processing of waste carpets into useful feedstocks for use in manufacturing. This study describes the experimental characterisation of a novel structural composite material that has been fabricated from waste carpets, and which is intended for use in low grade structural applications such as agricultural fencing. Details of the manufacturing process for the composites are described, as are the results of tensile and three-point bending tests, and the observed failure modes post-testing. In addition, Finite Element (FE) analysis was used to simulate the structural behaviour of fencing posts and rails manufactured from the carpet-based composite, and these results are compared with commercially available timber and PVC equivalent designs. Finally, structural analysis and design optimisation of the composite fencing was undertaken and this is used to demonstrate that from a mechanical property standpoint, the novel waste carpet structural composite may offer potential as an alternative to the timber and PVC materials typically used in such applications. Therefore, this study has demonstrated a practical approach for recycling carpet waste, which could lead to a substantial reduction in the volume of carpet waste discarded to landfill and subsequently yield both economic and environmental benefits.

Keywords

Carpet; Fencing; Waste; Mechanical properties; FE modelling; Composite

1. Introduction

Carpets, which are typically used as floor coverings, are composite materials that are difficult and costly to separate and reprocess at the end of their useful lives. This is because they are multilayer mixtures of different polymers and inorganic fillers. According to Carpet Recycling UK (Bird, 2014), 400,000 tonnes of carpets are sent to landfill in the UK annually. However, the landfill option is becoming increasingly impractical due to environmental impact considerations, reduced availability of sites, and increasing cost. More specifically, the landfill tax associated with the disposal of carpet waste to landfill was £24 per tonne in 2007 and increased to £84 per tonne in 2016 reflecting a 250% increase over nine years (Gardner, 2016). The UK government (2016) have also stated that the landfill tax will increase to £89 in 2018 to meet environmental objectives aimed at reducing the amount of waste produced and increasing the use of alternative waste management options. It is expected that, by 2025, carpet waste will be banned from UK landfill sites, because it is non-biodegradable and reduces their availability of landfill for other uses (Bird, 2014). Therefore, effective waste management is vital in attaining a sustainable environment. Indeed, the European Union's seventh framework programme aims to find innovative ways of utilising waste as a resource (European Union, 2010). Furthermore, as one tonne of recycled carpet waste saves 4.2 tonnes of CO_2 emissions (Carpet Recycling UK, 2010, Department for Environment Food and Rural Affairs, 2011), annual estimate savings of 1,680,000 tonnes of CO_2 emissions (based on 400,000 tonnes being sent to landfill annually in the UK) potentially could be achieved through the sustainable recycling of carpet waste in the UK.

A typical carpet consists of four layers: face fibre, primary backing, adhesive and secondary backing (see Figure 1), with approximate component percentages of 46 %, 6 %, 4 % and 44 % by weight, respectively (Vaidyanathan et al., 2013). In addition, post-consumer waste carpets typically contains dirt, chemicals and other materials, which accumulate in-service and make them about 30 % heavier than new carpets (Mihut et al., 2001).

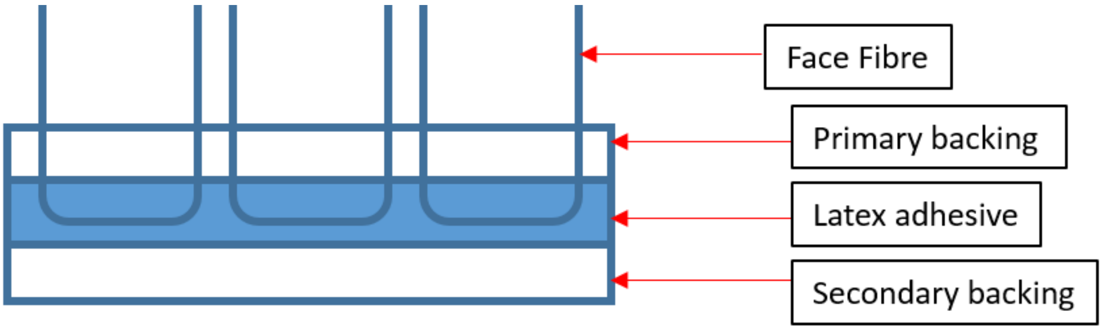

Figure 1: Typical construction of carpet

The face fibre top layer can either be nylon, polypropylene, polyethylene terephthalate (PET), mixed synthetics or natural fibres such as wool, cotton and jute (Jain et al., 2012). The primary backing is the layer through which the yarns of the face fibres pass and elastomeric adhesive is applied to the underside of the primary backing to hold the face fibres in place (The Carpet and Rug Institute, 2003). The elastomeric adhesive is typically made of styrene butadiene rubber (SBR), which can be filled with inorganic materials such as calcium carbonate ($CaCO_3$) or barium sulphate ($BaSO_4$) (Mihut et al., 2001). The secondary backing is the layer bonded to the back of the carpet pile. The primary and secondary backings can be made of polypropylene, nylon, polyurethane or jute (Miraftab and Mirzababaei, 2009). According to Helms and Hervani (2006), nylon and polypropylene are the most commonly used materials for the backings and face fibres of carpets.

Recently, the authors carried out a review of different carpet waste processing options in the UK, and also reported on the fabrication and mechanical properties of carpet based composites (Sotayo et al., 2015). This review highlighted that there are studies (Zhang et al., 1999, Gowayed et al., 1995) that have shown the potential of carpet waste being used as a raw material in the fabrication of structural composites and thereby diverting them from landfill and incineration options. However, there are limitations with these different processing options, which have focussed mainly on carpets with synthetic/man-made face fibres and/or the utilisation of only a fraction/layer of the carpet (i.e. face fibres, backing layers). In addition, some of the processes involved the mechanical separation of the carpets' constituents, costly fibre reprocessing procedures (i.e. depolymerisation), and the addition of glass fibres, all of which increase manufacturing processes, and hence, increase production cost.

Given the challenges associated with carpet recycling reported in Sotayo et al. (2015), this paper forms part of the broader objective, namely to recycle carpet waste via the sustainable development and experimental characterisation of novel waste carpet structural composites for use in fencing and other structural applications. Hence, the paper explores a manufacturing process which excludes a second phase (addition of glass fibres), mechanical separation, and fibre reprocessing, but includes carpets with both synthetic and natural fibres. An aim of this approach is to explore the viability of replacing common fencing materials (timber and PVC) with such carpet derived composites. Through this, carpet recycling could lead to economic benefits and a significant positive impact on the environment by reducing greenhouse gas emissions, preserving natural resources (i.e. non-renewable fossil fuel), decreasing deforestation and diverting carpet waste from landfill and incineration.

This paper reports details of the manufacture and experimentally derived mechanical properties of waste carpet structural composites, and uses the measured properties to computationally model the expected load-deformation response of a fencing structure. Via structural analysis and design optimisation, a composite fence structure having similar load-deformation response to conventional PVC and timber fences is proposed. Details of the manufacturing process are described and statistical analyses and failure modes (via Scanning Electron Microscopy (SEM) analysis) of the composite test-pieces are reported. It is concluded that the results of the investigation provide useful insight and understanding of the mechanical properties of novel waste carpet structural composites, and their suitability for use as alternatives to timber and PVC fencing.

2. Manufacturing Process for Waste Carpet Structural Composites

Post-consumer waste carpets were sorted according to their face fibres using a Thermo Scientific microPHAZIR PC handheld Near-Infrared (NIR) analyzer (Thermo Scientific, 2010) into three different categories: (a) Waste carpets constituted from polypropylene face fibres; (b) Waste carpets constituted from mixed synthetic face fibres (polypropylene, PET and nylon fibre blends); and (c) Waste carpets constituted from wool face fibres. The waste carpets were then separately shredded in a UNTHA VR140 granulator with a 40 mm screen. From these granulated carpet feedstocks, four different formulations of carpet feedstock composites (Composite C_PP; C_PPW; C_SF and C_SFW) were fabricated, as detailed in Table 1.

Table 1: Description of the four formulations of the waste carpet structural composites

Label	Composition
Composite C_PP	100 wt.% waste carpets with polypropylene face fibres
Composite C_PPW	50 wt. % waste carpets with polypropylene face fibres and 50 wt. % waste carpets with wool face fibres
Composite C_SF	100 wt. % waste carpets with synthetic face fibres
Composite C_SFW	50 wt. % waste carpets with synthetic face fibres and 50 wt. % waste carpets with wool face fibres

A 1kg batch size of shredded carpet waste was mixed in a Banbury mixer until the temperature in the barrel reached 150 ^{o}C. The blended mixture was then placed in a steel mould of size 300 mm x 150 mm x 10 mm, and the mould was subjected to a pressure of 14 MPa in a hydraulic press for five minutes at ambient temperature. Figure 2 shows a flow diagram of the processes used for fabricating the waste carpet structural composites.

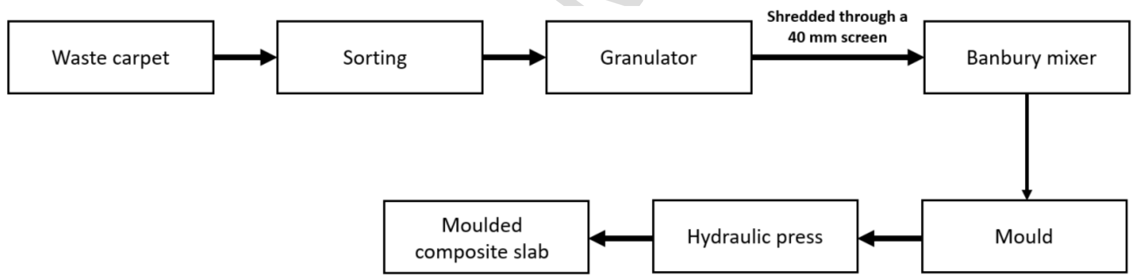

Figure 2: Flow diagram showing the processes involved in the manufacture of the waste carpet structural composites

Once cool, rectangular test-pieces of size 39 mm x 11 mm x 293 mm were cut from the compression moulded composite slabs (see Figure 3). Upon unloading of the sample from the hydraulic press, thickness expansion (i.e. spring back of about 1 mm) occurred. The post-compression moulded samples demonstrated visible defects that included flow lines, voids and regions of surface profile irregularity (roughness), reflecting the inhomogeneous nature of the carpet feedstocks, and the broad range of melting temperatures of the constituent fibres. Such defects are common in materials made from recycled waste (Waghorn and

Sapsford, 2017, Singh et al., 2016) . Therefore, post-processing (i.e. machining) of the samples would be required for the production of a good surface finish.

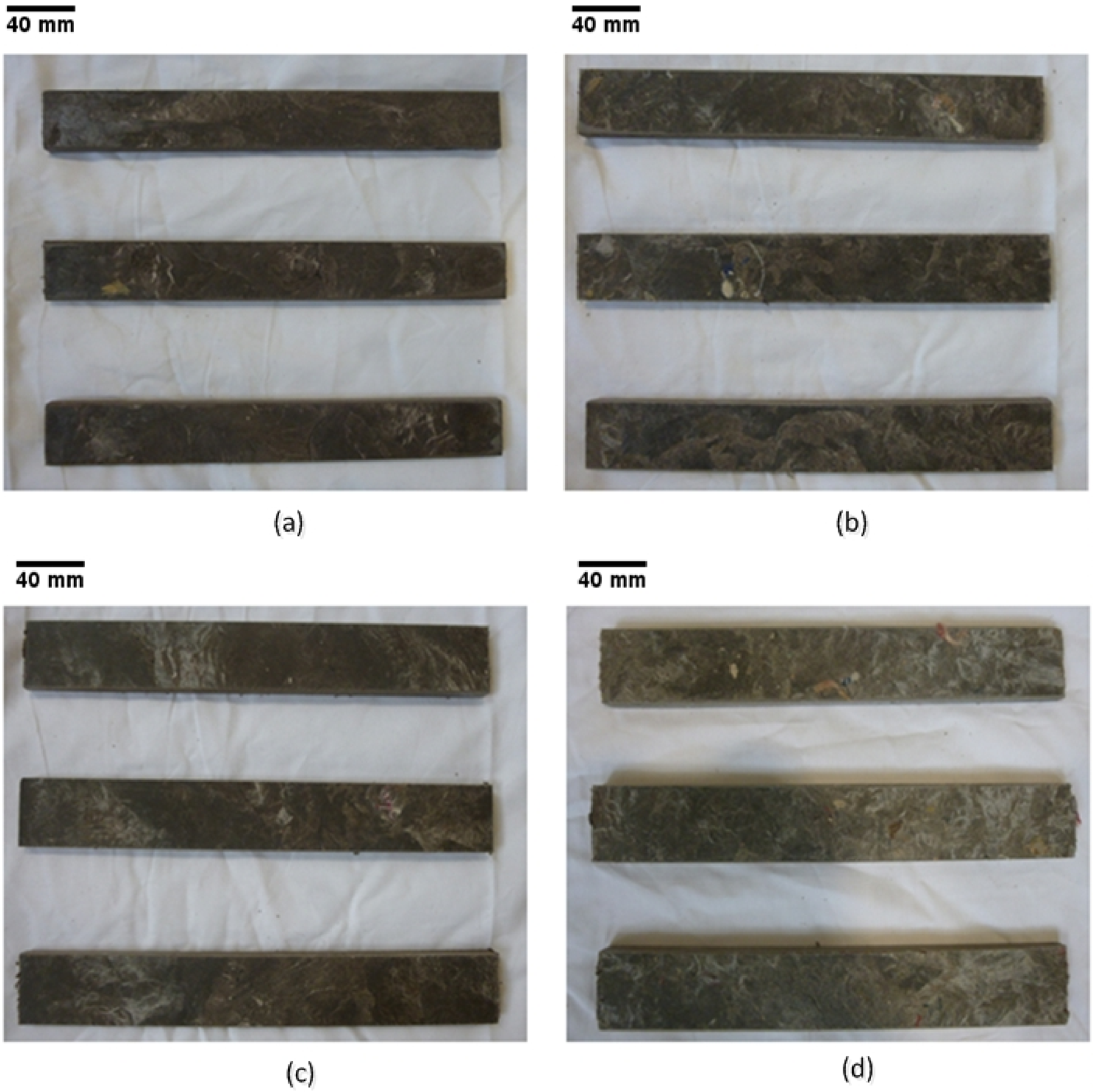

Figure 3: Images of the waste carpet structural composites: (a) C_PP (b) C_PPW (c) C_SF (d) C_SFW

Of note, Composite C_SFW was observed to contain a significant fraction of un-melted fibres/fibre-rich phase. At the processing temperature within the Banbury mixer of 150 ^{o}C, neither the wool fibres nor the thermosetting elastomeric adhesive (SBR) melted. In contrast, the melting temperature of the polypropylene fibres is about 160 ^{o}C, which is significantly lower than the melting temperatures of the other synthetic fibres of nylon (215 – 265 ^{o}C) and PET (256 – 268 ^{o}C) (Palenik, 1999). Hence, for all the composites, the post-compression moulded form was that of a polypropylene matrix, within which was dispersed mixed second phases of elastomeric adhesive, inorganic fillers ($CaCO_3$ and $BaSO_4$), dirt particles and other carpet fibres (nylon, PET, wool).

3. Experimental Characterisation

3.1. Experimental Setup, Instrumentation and Test Procedure for the Three-Point Bending Tests

Three-point bending tests were carried out on the moulded composite samples. Figure 4a shows a sketch of the three-point beam bending test setup and Figure 4b shows a sketch of the specimen cross-section. Table 2 gives the average dimensions of the beams tested in three-point bending. Also, the span to depth ratio of the beam in bending is greater than 16, i.e. sufficiently large for shear deflection effects to be ignored.

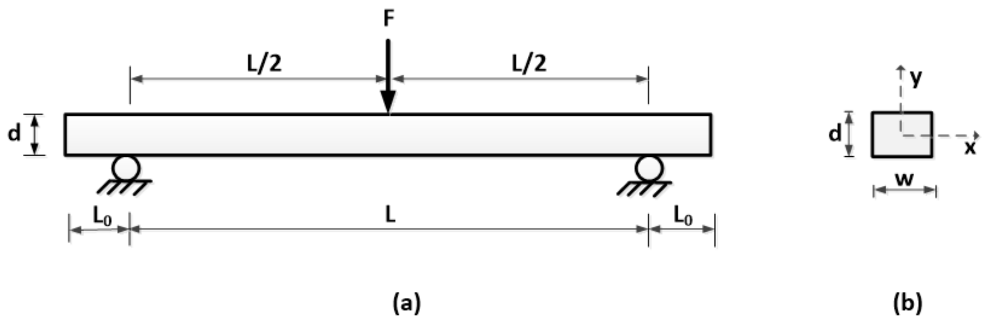

Figure 4: Sketches of the three-point bending test setup: (a) Side-view and (b) Cross-section view

Each of the four formulations of the novel waste carpet structural composites (C_PP, C_PPW, C_SF and C_SFW) described in Table 1 were tested to determine their elastic flexural moduli and strengths.

Table 2: Dimensions of the waste carpet structural composite beams tested in three-point bending

Overall length [L + 2L_0] [mm]	Span [L] [mm]	Average width [w] [mm]	Average depth [d] [mm]	Support overhang [L_0] [mm]	Second moment of area about x-axis [mm^4]
293	240	39	11	26.5	4,326

The three-point bending tests were carried out at a crosshead displacement rate of 2 mm/min in a universal testing machine (Zwick Z020) with a load capacity of 20 kN. Figure 5 shows an image of Composite C_PP setup on the testing machine. The load and deflection data were recorded by a computer controlled data acquisition system.

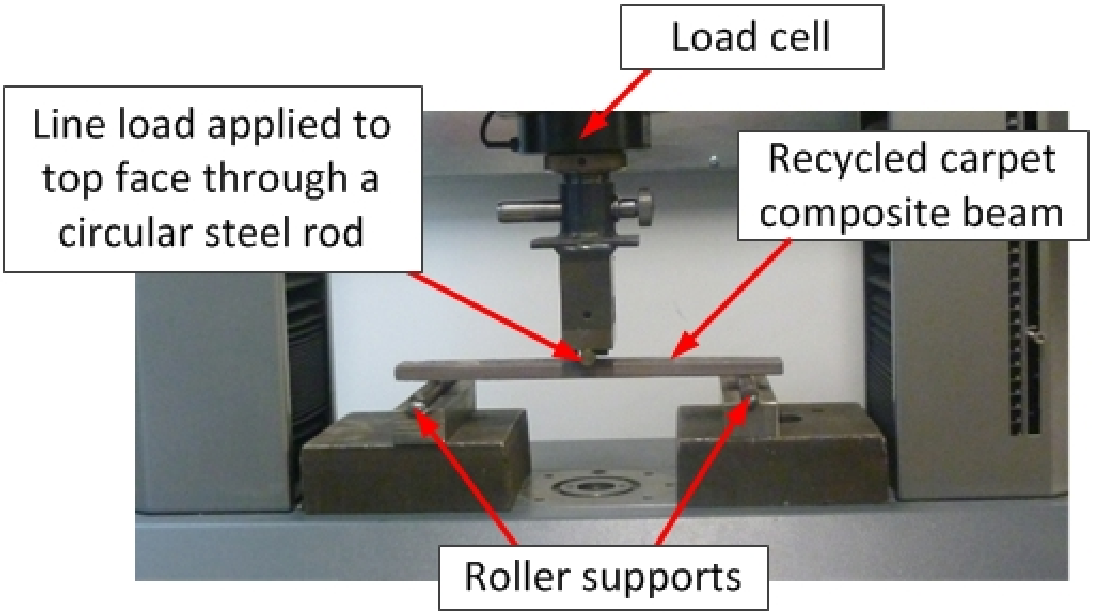

Figure 5: Image of Composite C_PP beam setup for three-point bending in a Zwick Z020 testing machine

3.2. Experimental Setup, Instrumentation and Test Procedure for the Uniaxial Tensile Tests

Uniaxial tensile tests were carried out on nominally identical waste carpet structural composites. As for the three-point bending tests, each of the four formulations of the novel waste carpet structural composites (C_PP, C_PPW, C_SF and C_SFW) were tested in uniaxial tension (see Table 1). Figure 6 shows sketches of the uniaxial test specimens, and their dimensions are given in Table 3.

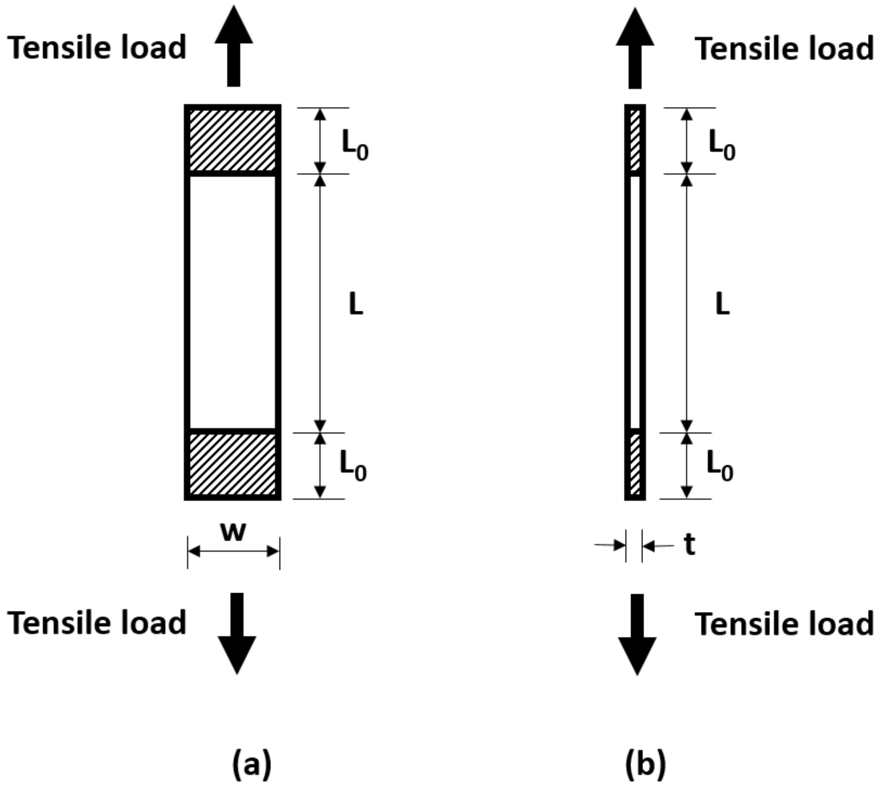

Figure 6: Sketches of a uniaxial tensile test specimen: (a) Front-view (b) Side-view

Table 3: Dimensions of the waste carpet structural composite tensile test specimens

Width [w] [mm]	Thickness [t] [mm]	Gauge length [L] [mm]	Grip length [L_0] [mm]
39	11	193	50

The specimens were tested in uniaxial loading using the same universal testing machine as described in Section 3.1, and operated at the same crosshead displacement rate. The experimental setup is shown in Figure 7. The loads applied to the uniaxial test specimens were recorded by the data acquisition system of the testing machine, whereas the longitudinal strains were recorded with a non-contact digital image correlation (DIC) system (Imetrum, Bristol, UK) (Imetrum), over a gauge length of 50 mm. A speckle pattern was applied to the tensile test specimens to facilitate adequate optical contrast for the DIC operation (see Figure 8).

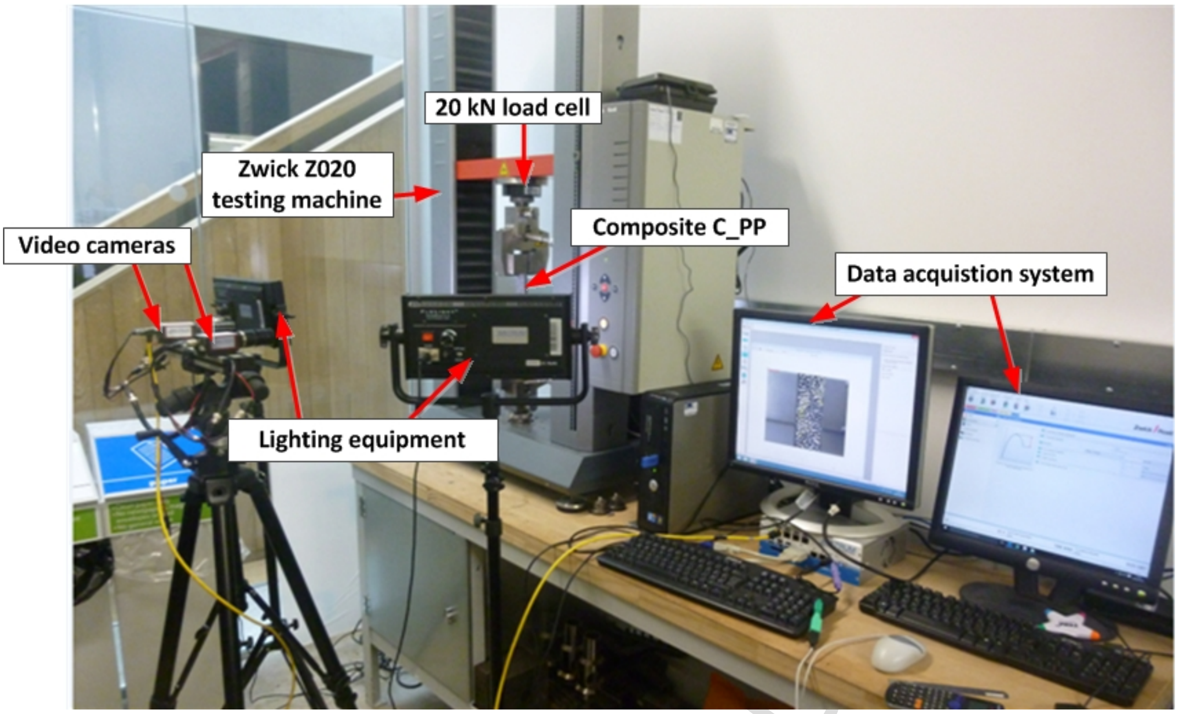

Figure 7: Image of the uniaxial tensile test setup on the Composite C_PP material

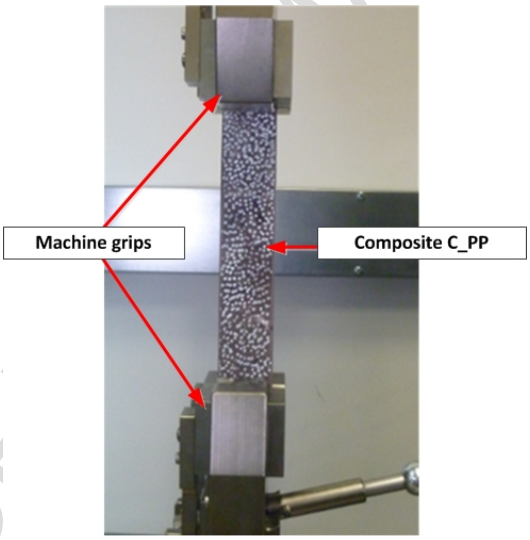

Figure 8: Uniaxial tensile test-piece showing speckle pattern needed for the DIC measurement of longitudinal strain

3.2.1. Setup for Scanning Electron Microscopy (SEM)

Backscatter Scanning Electron Microscopy (SEM) images were acquired via a Phenom G1 desktop SEM (Phenom-world, Eindhoven, The Netherlands) working at an accelerating voltage of 5 keV. In order to reduce surface charge, samples were sputter coated for 30 seconds prior to imaging using a SC7640 sputter coater (Quorum Technologies, Sussex, U.K.) fitted with a Gold/palladium (Au/Pd) sputter target. The magnification was 515x.

4. Experimental Results and Discussion

4.1. Results and Discussion of the Three-Point Bending Tests

Figure 9 shows the average load-centre deflection responses for five Composite C_PP beams when tested experimentally in three-point bending until failure. For all the samples, the load-deflection responses tended to change from linear to nonlinear for loads above 200 N. The load-centre deflection responses for Composite C_PP are also similar to those of Composite C_PPW, C_SF and C_SFW.

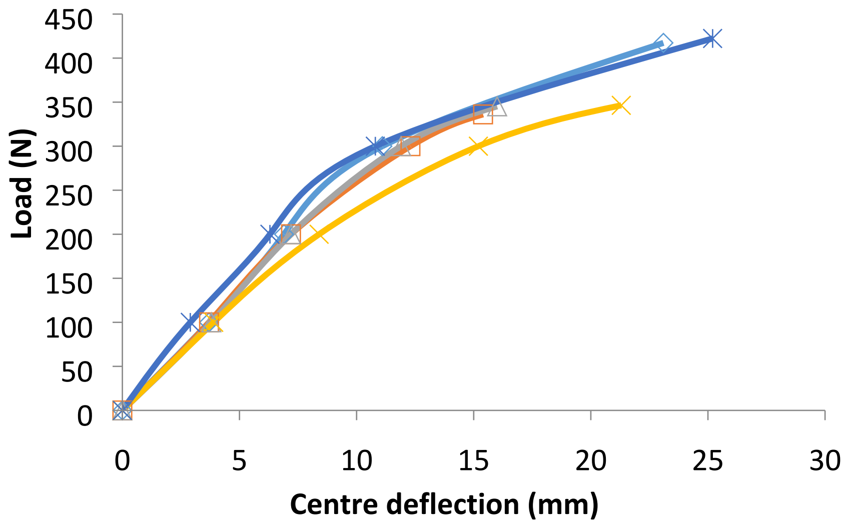

Figure 9: Load versus deflection plots for five Composite C_PP beams loaded in three-point bending to failure

The flexural moduli and flexural strengths obtained from the different composite formulations are shown in Figure 10 and Figure 11, respectively; the upper and lower bound values are also shown in the figures. The average flexural moduli for Composites C_PP and C_PPW were 2.3 GPa and 2.6 GPa, respectively. These values show that the addition of 50 wt. % waste carpets with wool face fibres to 50 wt. % waste carpets with polypropylene face fibres gave a 13 % increase in the average flexural modulus. The average flexural modulus for Composite C_SF was also 2.3 GPa (the same value as Composite C_PP). The addition of 50 wt. % waste carpets with wool face fibres to 50 wt. % waste carpets with synthetic face fibres also gave a 35 % increase in the average flexural modulus i.e. from 2.3 GPa to 3.1 GPa. These results show that the addition of waste carpets with wool face fibres to waste carpets with polypropylene face fibres or synthetic face fibres (i.e. polypropylene, nylon, PET) resulted in an increase in the flexural modulus.

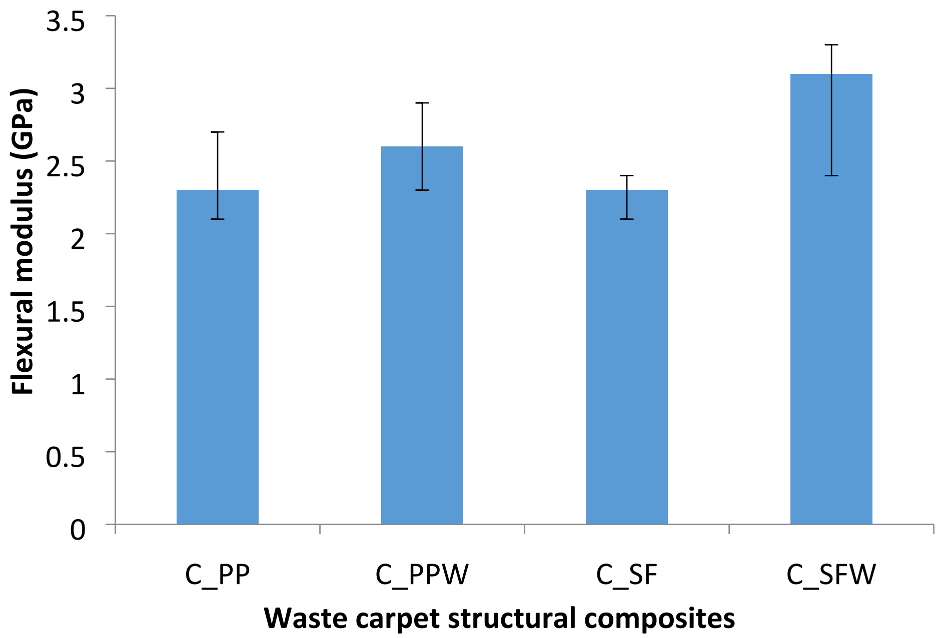

Figure 10: Comparison of the flexural modulus of the waste carpet structural composites

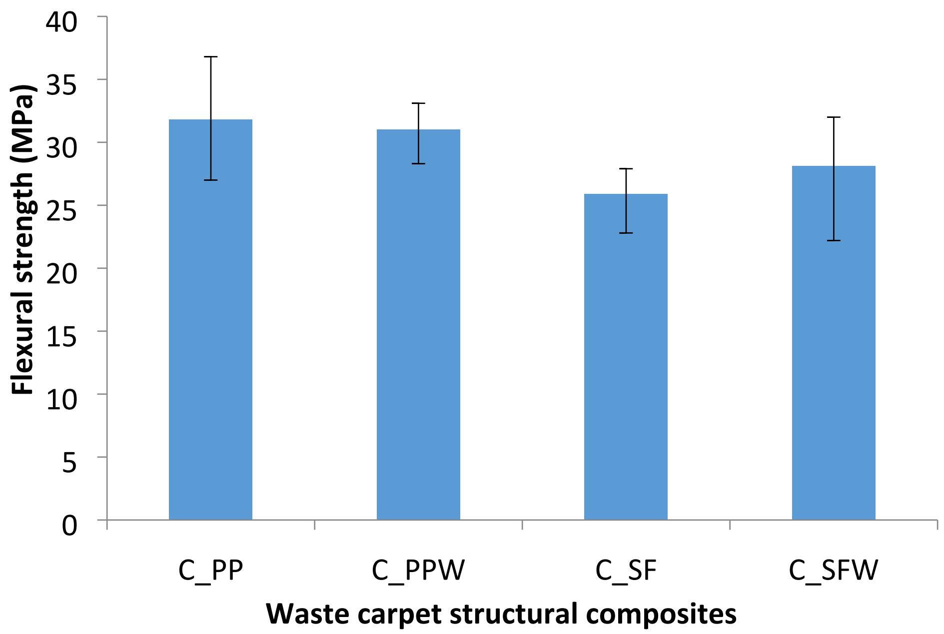

Figure 11: Comparison of the flexural strength of the waste carpet structural composites

The average flexural moduli, flexural strengths, standard deviations and coefficients of variation of the waste carpet structural composites tested in three-point bending are given in Table 4. The overall average flexural modulus was 2.6 GPa. The average flexural strength for Composite C_PP was 31.8 MPa which was the highest of the four formulations, whereas Composite C_SF had the lowest average flexural strength of 25.9 MPa. The average flexural strengths for Composite C_PP and C_PPW were 31.8 MPa and 31.0 MPa, respectively, which are almost equal. The overall average flexural strength for the waste carpet structural composites was 29.2 MPa (see Table 4).

Table 4: Average flexural moduli, average flexural strengths, standard deviations and coefficients of variation for the waste carpet structural composites

Label	Flexural modulus			Flexural strength		
	Average [GPa]	Standard deviation (SD) [GPa]	Coefficient of variation [%]	Average [MPa]	Standard deviation (SD) [MPa]	Coefficient of variation [%]
C_PP	2.3	0.2	8.0	31.8	3.8	12.1
C_PPW	2.6	0.2	6.6	31.0	1.8	5.8
C_SF	2.3	0.1	5.5	25.9	2.0	7.8
C_SFW	3.1	0.3	10.4	28.1	3.9	14.0
Overall average flexural modulus					**2.6 GPa**	
Overall average flexural strength					**29.2 MPa**	

4.2. Results and Discussion of the Uniaxial Tensile Tests

Figure 12 shows the tensile load-extension plots for the Composite C_SFW specimens. The results showed good repeatability, with an initial linear response, which became nonlinear after about 4000 N. The tensile load-extension plots for Composite C_PP, C_PPW and C_SFW specimens are similar to that shown in Figure 12, though, of course, the magnitudes were different. All the specimens failed in a brittle manner and Figure 13 shows an image of the failure mode for a Composite C_PP specimen in uniaxial tension.

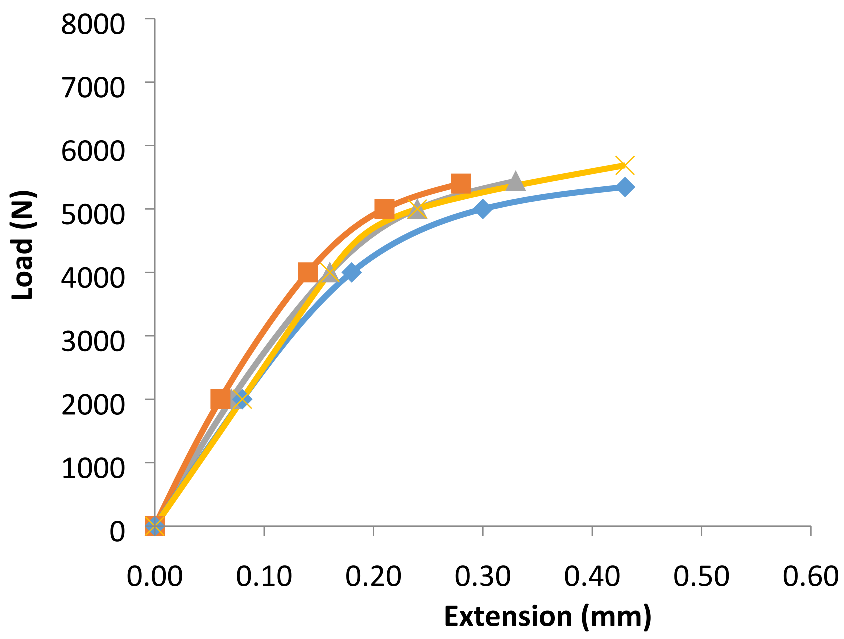

Figure 12: Tensile load versus extension plots for four Composite C_SFW specimens

Table 5 gives the average tensile strengths and moduli for the waste carpet structural composites. The standard deviations and coefficients of variation are also presented in Table 5. Furthermore, their tensile moduli and strengths are compared in Figure 14 and Figure 15, respectively; the upper and lower bounds are also shown in the Figures.

The average tensile modulus for Composites C_PP and C_PPW was 2.9 GPa and 2.7 GPa, respectively. These values show that the addition of 50 wt. % waste carpets with wool face fibres to 50 wt. % waste carpets with polypropylene face fibres resulted in a 7 % reduction in the average tensile modulus. On the other hand, the average tensile modulus for Composites C_SF and C_SFW was 2.3 and 2.8 GPa, respectively, reflecting an approximate 22 % increase in tensile modulus. The overall average tensile modulus for the uniaxial tensile test coupons was 2.7 GPa, and the corresponding coefficient of variation ranged from 8.4 – 14.0 %.

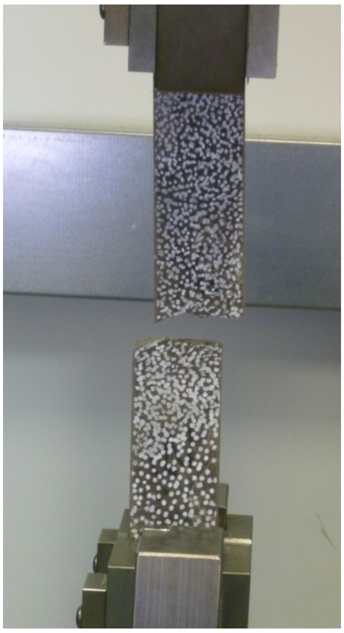

Figure 13: Failure mode of a waste carpet structural composite specimen (C_PP) in uniaxial tension

Table 5: Average tensile moduli, average tensile strengths, standard deviations and coefficients of variation for the waste carpet structural composites

Label	**Tensile modulus**			**Tensile strength**		
	Average [GPa]	**Standard deviation (SD) [GPa]**	**Coefficient of variation [%]**	**Average [MPa]**	**Standard deviation (SD) [MPa]**	**Coefficient of variation [%]**
C_PP	2.9	0.2	8.4	17.8	1.5	8.7
C_PPW	2.7	0.3	10.2	14.2	1.4	9.9
C_SF	2.3	0.3	14.0	12.8	1.2	9.5
C_SFW	2.8	0.3	12.3	13.2	0.6	4.2
Overall average tensile modulus					**2.7 GPa**	
Overall average tensile strength					**14.5 MPa**	

Of the four formulations, Composite C_PP had the highest average tensile strength of 17.8 MPa, whereas Composite C_SF had the lowest average tensile strength of 12.8 MPa. The addition of 50 wt. % waste carpets with wool face fibres to 50 wt. % waste carpets with polypropylene face fibres resulted in an approximate 20 % reduction in the tensile strength (cf. Composite C_PP and C_PPW in Figure 15). The average tensile strength for Composite C_SFW was 3 % greater than that of Composite C_SF. The overall average tensile strength for the uniaxial tensile test coupons was 14.5 MPa, and the coefficient of variation ranged from 4.2 – 9.9 %.

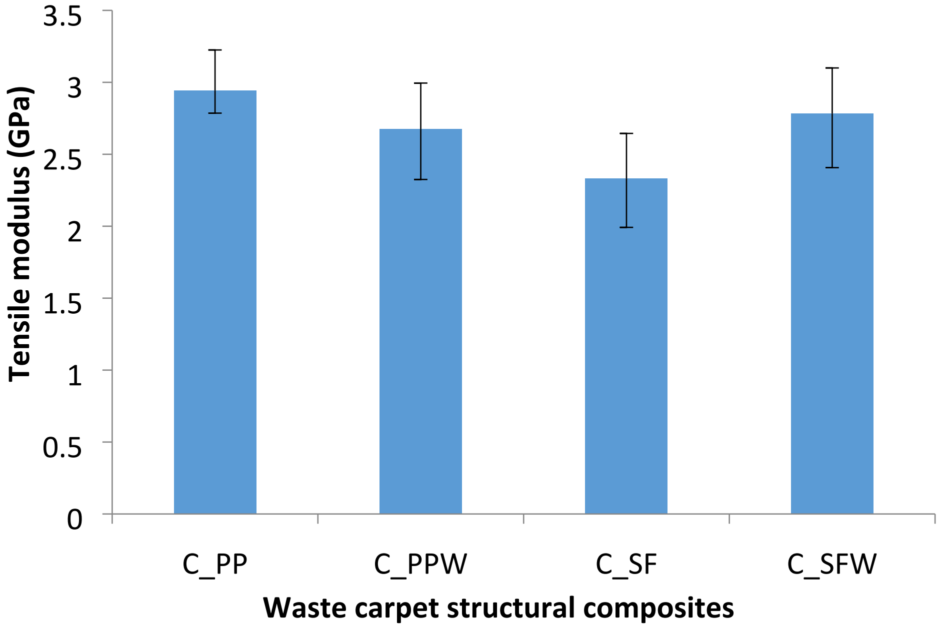

Figure 14: Comparison of the tensile modulus of the waste carpet structural composites

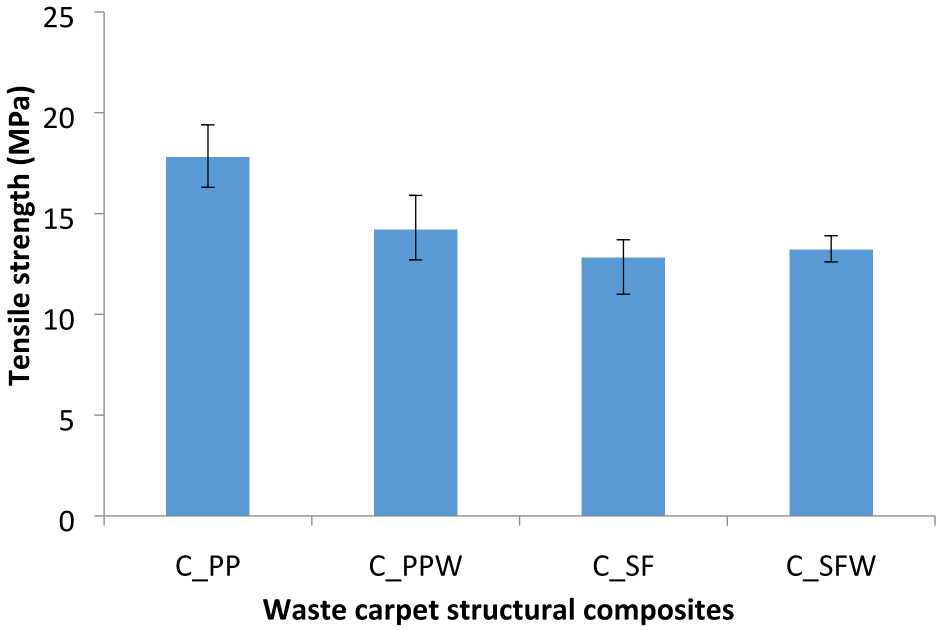

Figure 15: Comparison of the tensile strength of the waste carpet structural composites

4.2.1. Failure Modes and Scanning Electron Microscopy (SEM) Analysis

As mentioned earlier, the waste carpet structural composites failed in a brittle manner. Representative images of fracture surfaces of the waste carpet structural composites (C_PP, C_PPW, C_SF and C_SFW) and their respective Scanning Electron Microscopy (SEM) images are given in Figure 16 – Figure 19.

(a)

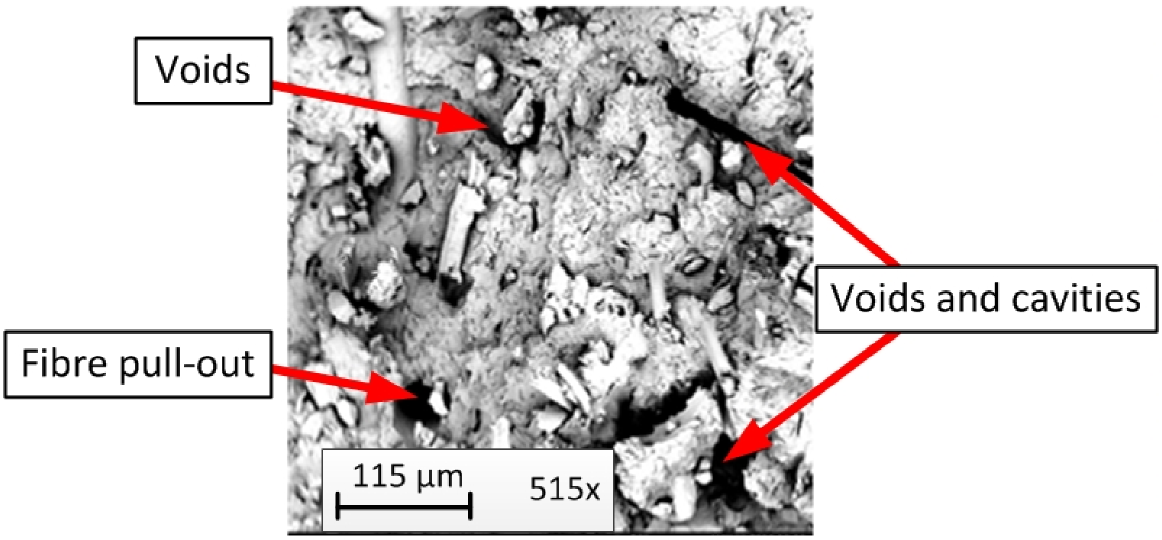

(b)

Figure 16: Composite C_PP specimen failed in uniaxial tension: (a) Cross-section view of the fracture surface (b) SEM image of the fracture surface

(a)

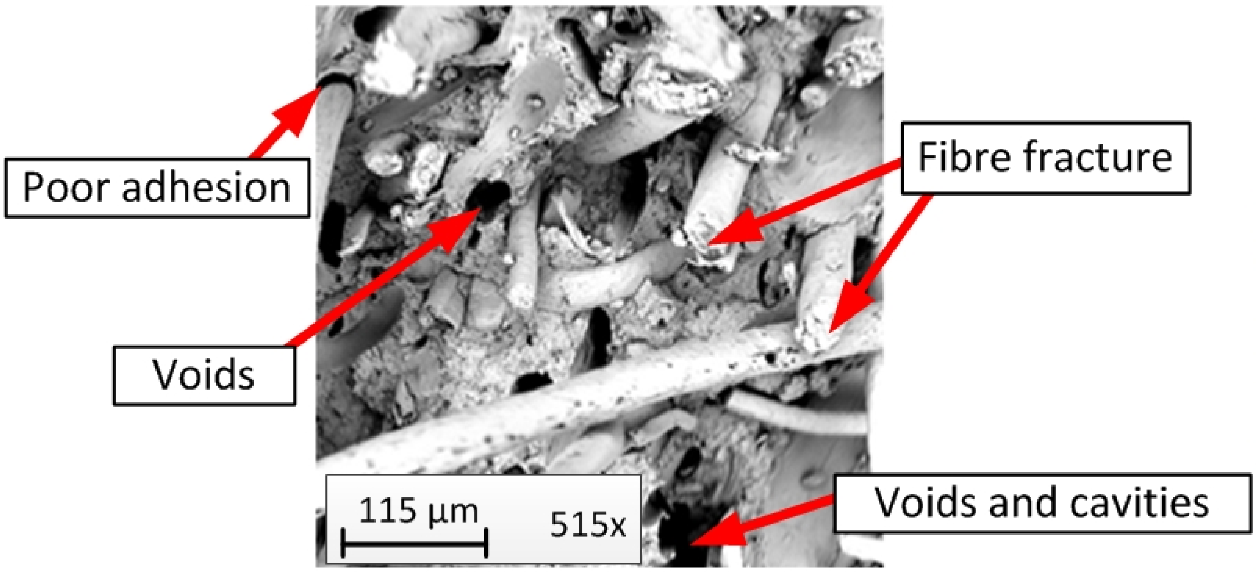

(b)

Figure 17: Composite C_PPW specimen failed in uniaxial tension: (a) Cross-section view of the fracture surface (b) SEM image of the fracture surface

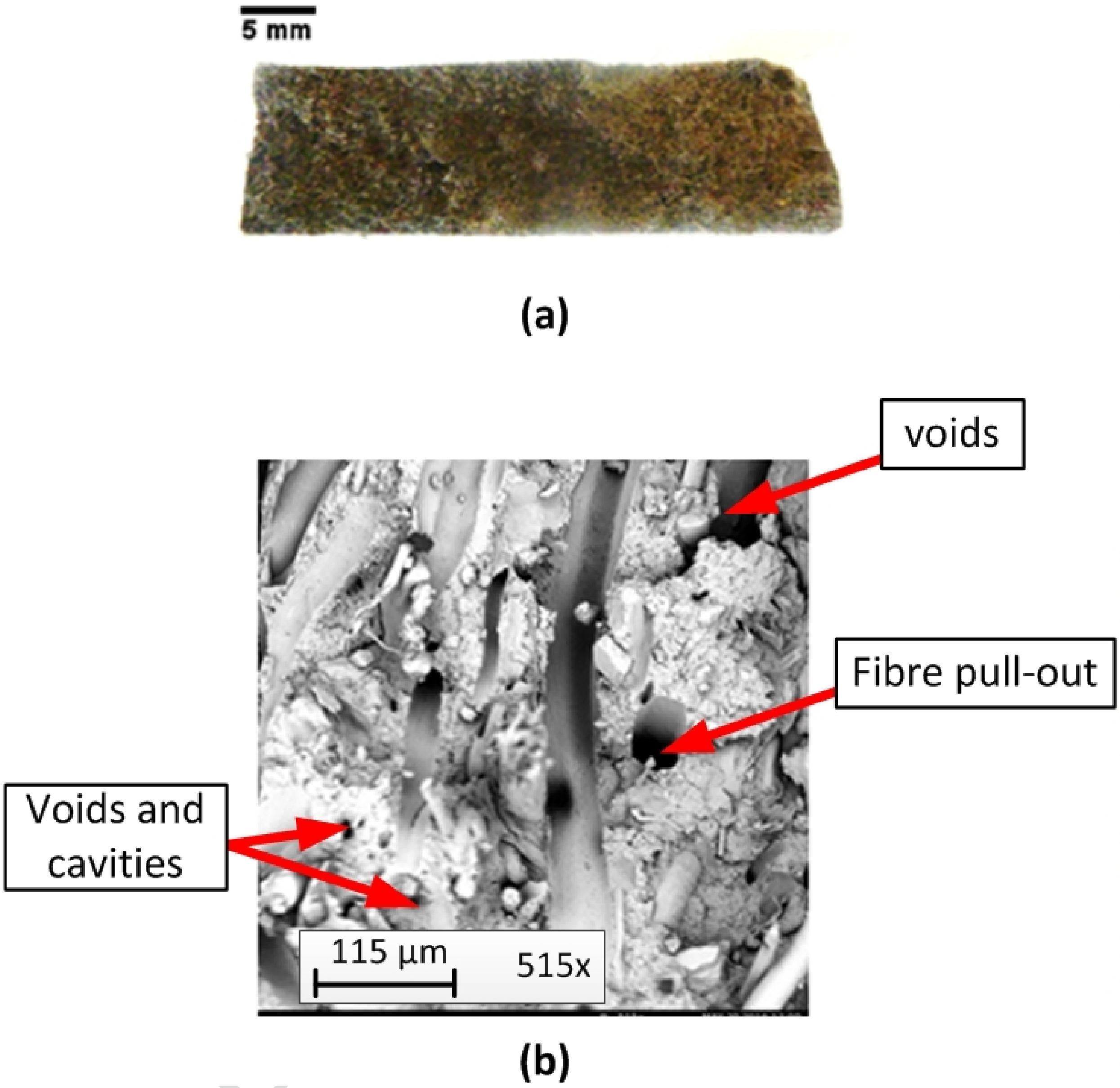

Figure 18: Composite C_SF specimen failed in uniaxial tension: (a) Cross-section view of the fracture surface (b) SEM image of the fracture surface

(a)

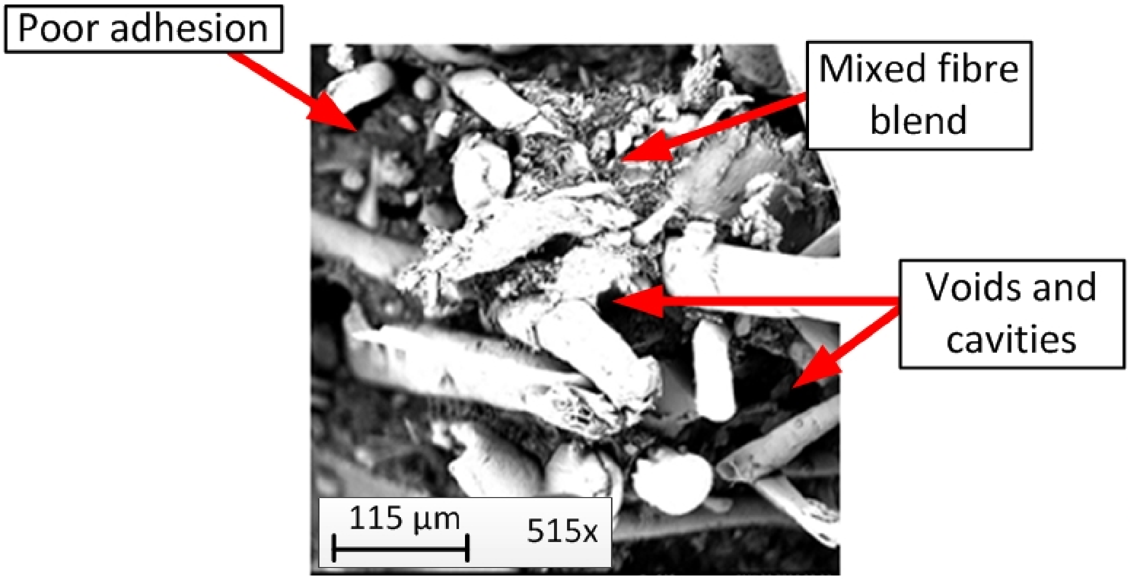

(b)

Figure 19: Composite C_SFW specimen failed in uniaxial tension: (a) Cross-section view of the fracture surface (b) SEM image of the fracture surface

It is evident from the SEM images that Composites C_PPW and C_SFW (both with carpet waste with wool face fibres) had a greater quantity of exposed fibres compared to Composites C_PP and C_SF (without carpet waste with wool face fibres). All the SEM images show evidence of voids, cavities, fibre pull-out and exposed fibres. Furthermore, the melt blended mixture contained different immiscible polymers (i.e. nylon and polypropylene), dirt particles, fillers, chemicals and impurities (typical of post-consumer carpet waste) which may have contributed to the defects shown in Figure 16 – Figure 19.

5. Finite Element (FE) Modelling of Novel Carpet Structural Composite Fencing Structures

This section describes the Finite Element (FE) modelling and analysis of a fencing structure modelled as constituted from material having elastic properties matching that obtained from the moulded composites, as reported in Section 3.2.1. At 2.6 GPa (see Table 4), the overall average flexural modulus for the waste carpet structural composite is around 25 % that of timber (10 GPa) and very close to that of PVC (2.7 GPa) (Sotayo et al., 2016, Sotayo et al., 2017). Recently, the authors (Sotayo et al., 2016, Sotayo et al., 2017) carried out experimental load tests on timber and PVC fencing structures, the results of which act as benchmark data for the analysis in this paper. From that work, the transverse stiffnesses of the two-bay timber and PVC fences were measured to be 50.7 N/mm and 14.0 N/mm, respectively.

FE analyses were carried out on two-bay timber fence FE model developed using the ANSYS software, details of which are reported in Sotayo et al. (2016). The comparisons and validations of the aforementioned timber FE model with the experimental test results have shown that the FE model can be used with confidence to investigate the load-deformation response of a fencing structure comprised of novel structural composites. Thus, FE analyses were carried out and evaluated using the elastic properties of the waste carpet structural composites and the geometric properties of the two-bay timber fence. Thereafter, geometric optimisations and structural analyses via changes to the rectangular cross-sections of the posts and rails and their overall layout, were carried out and evaluated to achieve stiffness properties similar to those of the previous timber and PVC fencing structures. The overall geometry and post/rail cross-section dimensions for the two-bay waste carpet structural composite fence FE model are given in Figure 20 and Table 6.

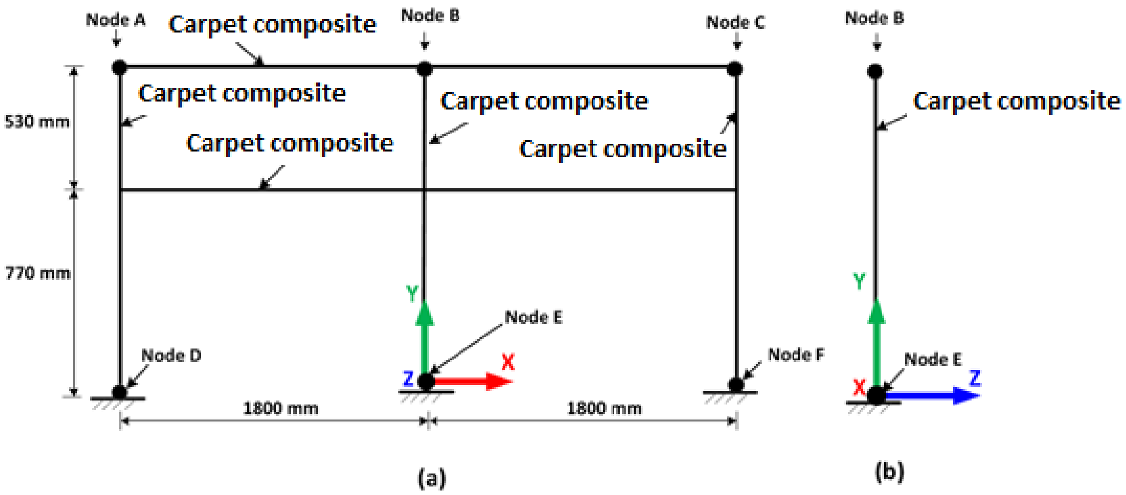

Figure 20: Overall geometry of the two-bay waste carpet structural composite fence FE model: (a) Front-view (b) Edge-view from Node B to Node C

As the two-bay fence was loaded to produce transverse bending under service loading, only the longitudinal elastic properties of the posts and rails significantly affected the FE simulation results. For simplicity, all of the fence components were modelled as isotropic linear elastic materials, and for computational efficiency, BEAM188 elements were used to represent the posts and rails, and MPC184 elements were used to represent the joints at the base of the posts. The rotational stiffness with respect to the x-axis was 3 x 10^5 Nm/rad and the other five nodal displacements were set to zero at the base joints (see Nodes D – F in Figure 20a). A load of 1400 N was applied at Node B (top of the centre post) in the negative z-direction (see Figure 20). The elastic flexural modulus and Poisson's ratio used for the waste carpet structural composite posts and rails were 2.6 GPa and 0.3, respectively.

Table 6: Details of the waste carpet structural composite posts and rails used in the FE model

Post/rail	Width [mm]	Depth [mm]	Second moment of area about plane of flexure [mm^4]	Flexural modulus [GPa]	Poisson's ratio
Post	122	71	3,638,762	2.6	0.3
Rail	93	37	392,561		

The FE analysis showed a deflection of 80.4 mm at the top of the centre post, based on an applied load of 1400 N at Node B (see Figure 20). Based on the deflection and load applied at the top of the centre post, the relative transverse stiffness of the two-bay waste carpet structural composite fence was evaluated to be 17.4 N/mm. The aforementioned relative transverse stiffness of the two-bay waste carpet structural composite fence FE model was compared with the experimentally derived transverse stiffnesses of the two-bay timber and PVC fences reported in Sotayo et al. (2016) and Sotayo et al. (2017), respectively and are shown in Figure 21. The results show that the relative transverse stiffness of the two-bay waste carpet structural composite fence is 24.3 % greater than a similar PVC fence. On the other hand, it is evident that the relative transverse stiffness of the two-bay timber fence is about three times greater than a similar waste carpet structural composite fence. This was expected as the experimentally derived flexural moduli of the timber posts and rails varied from 8.1 GPa – 13.5 GPa (Sotayo et al., 2016), and were significantly greater than the average flexural modulus of the waste carpet structural composite (2.6 GPa).

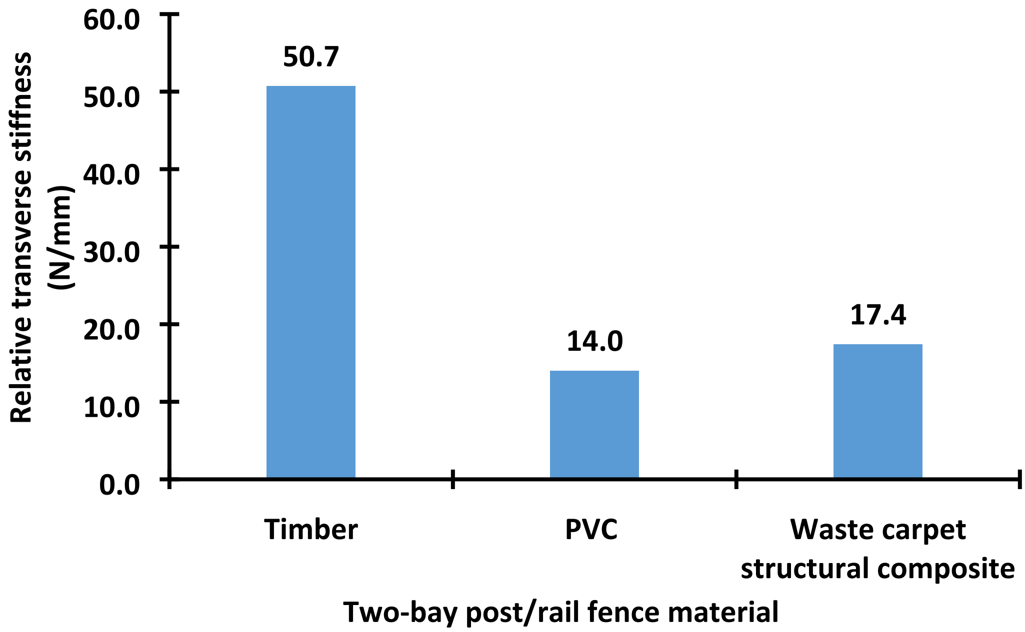

Figure 21: Comparison of the relative transverse stiffnesses of two-bay timber, PVC and the waste carpet structural composite fences

5.1. Geometric Optimisation of the Cross-Sections of the Waste Carpet Structural Composite Posts and Rails

As a result of the relatively lower transverse stiffness of the two-bay waste carpet structural composite fence compared to the timber fence, this section focusses on the design optimisation of the waste carpet structural composite posts and rails and the overall geometric layout of the structure to achieve a transverse stiffness similar to that of the timber fence. An increase in the second moment of area of the members of a structure gives an increase in its overall stiffness. Therefore, the second moment of area about the plane of flexure for the waste carpet structural composite posts and rails were increased by increasing the depth of their respective cross-sections, whilst their widths remained constant (see Figure 22). The depths of the waste carpet structural composite posts and rails were increased by a factor of two; the depth of the former was increased from 71 to 142 mm, and the latter from to 37 to 74 mm (in increments of 5 mm). It should be appreciated that the depths of the posts and rails were increased independently, not simultaneously.

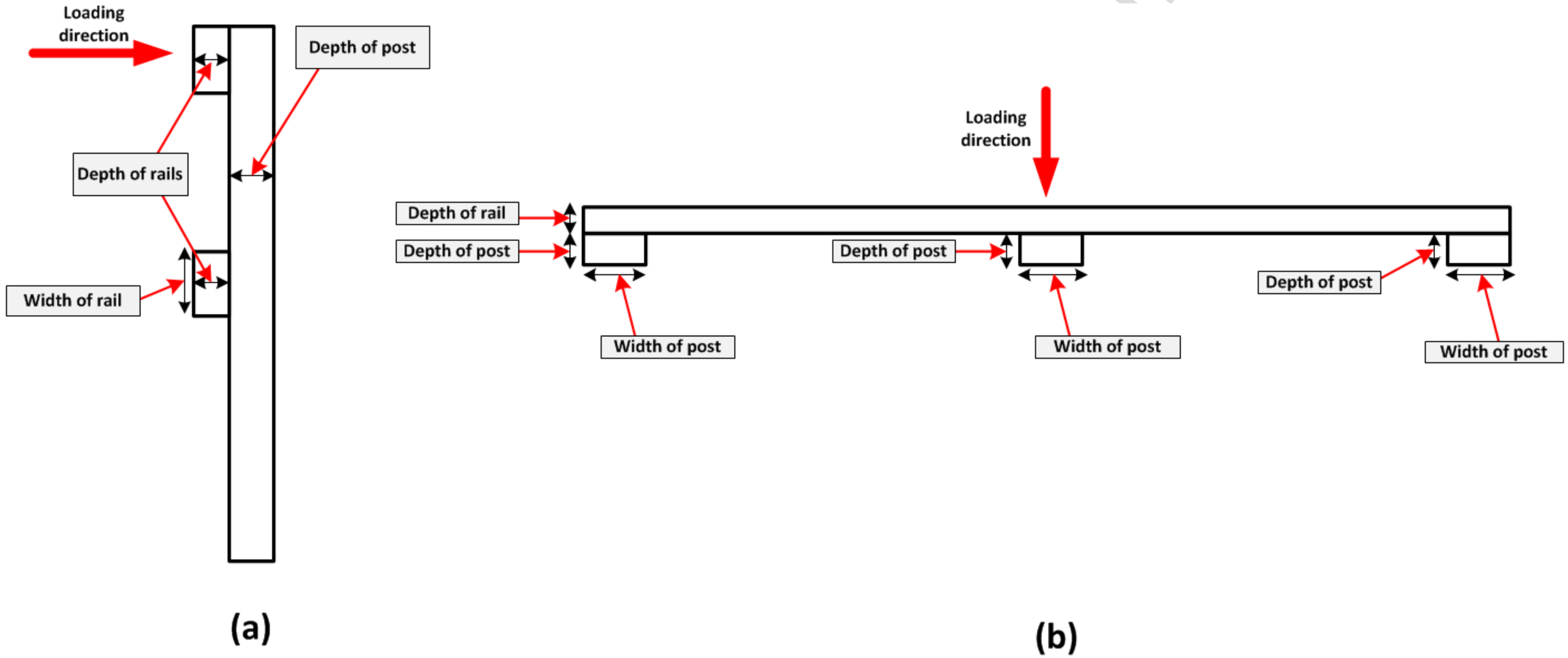

Figure 22: Sketches showing the depths and widths of the waste carpet structural composite posts and rails that were optimised: (a) Edge-view and (b) Plan-view

Figure 23 shows a plot of the maximum deflection (at Node B, see Figure 20) against the depths of the waste carpet structural composite posts and rails based on an applied load of 1400 N at the top of the centre post. Figure 23 also shows that the maximum deflection gradually decreases towards an asymptotic value as the depths of the respective posts and rails increases.

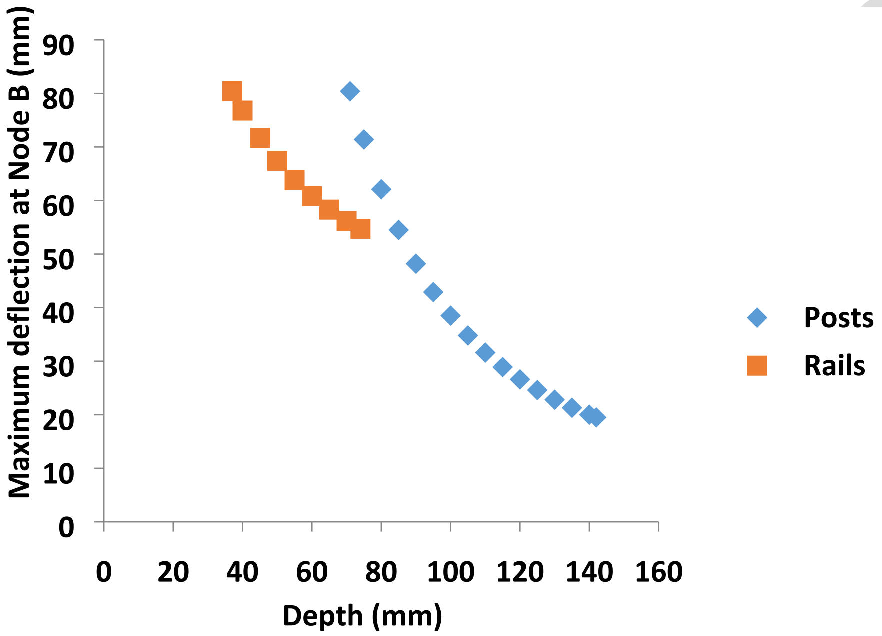

Figure 23: A plot of the maximum deflection against the depths of the waste carpet structural composite posts and rails based on an applied load of 1400 N at the top of the centre post

The analyses show that doubling the depths of each of the three posts of the two-bay fence reduced the maximum deflection from 80.4 to 19.5 mm, whereas doubling the depths of the two rails reduced the maximum deflection from 80.4 to 54.7 mm. These analyses demonstrate that an increase in the depths of the respective posts and rails by a factor of 2 reduces the maximum deflections by 76 % and 32 %, respectively (see Figure 23). Hence, increasing the second moment of area of the posts leads to a greater reduction in the maximum deflection compared to increasing that of the rails. Therefore, increasing the flexural stiffnesses of the posts rather than the rails leads to a stiffer fencing structure.

5.2. Structural Optimisation through an Increase in the Number of the Waste Carpet Structural Composite Posts and Rails of the Fencing Structure

An investigation was carried out into the effect of increasing the number of the posts and rails on the maximum deflection of the fencing structure when a load of 1400 N was applied at the top of the centre post. Sketches of the different geometric layouts comprising 2 – 5 rails and 3 – 9 posts are given in Figure 24 and Figure 25, respectively. Figure 24(a) – (d) were two-bay fencing structures with two, three, four and five rails, respectively. It should be noted that the spacing between the rails was reduced from 530 mm (from Figure 20) to 300 mm (see Figure 24); this was done so that the centre-to-centre spacing between the five rails was 300 mm. However, the adjustment of the geometric layout from Figure 20 to Figure 24a only resulted in a maximum deflection of 78 mm, i.e. only 3 % lower than the former. On the other hand, although the fencing structure's overall dimensions remained 1300 by 3600 mm, the geometric layouts given in Figure 25 had different numbers of bays, ranging from two – eight. The cross-sections of the waste carpet structural composite posts and rails were kept the same as those in Table 6.

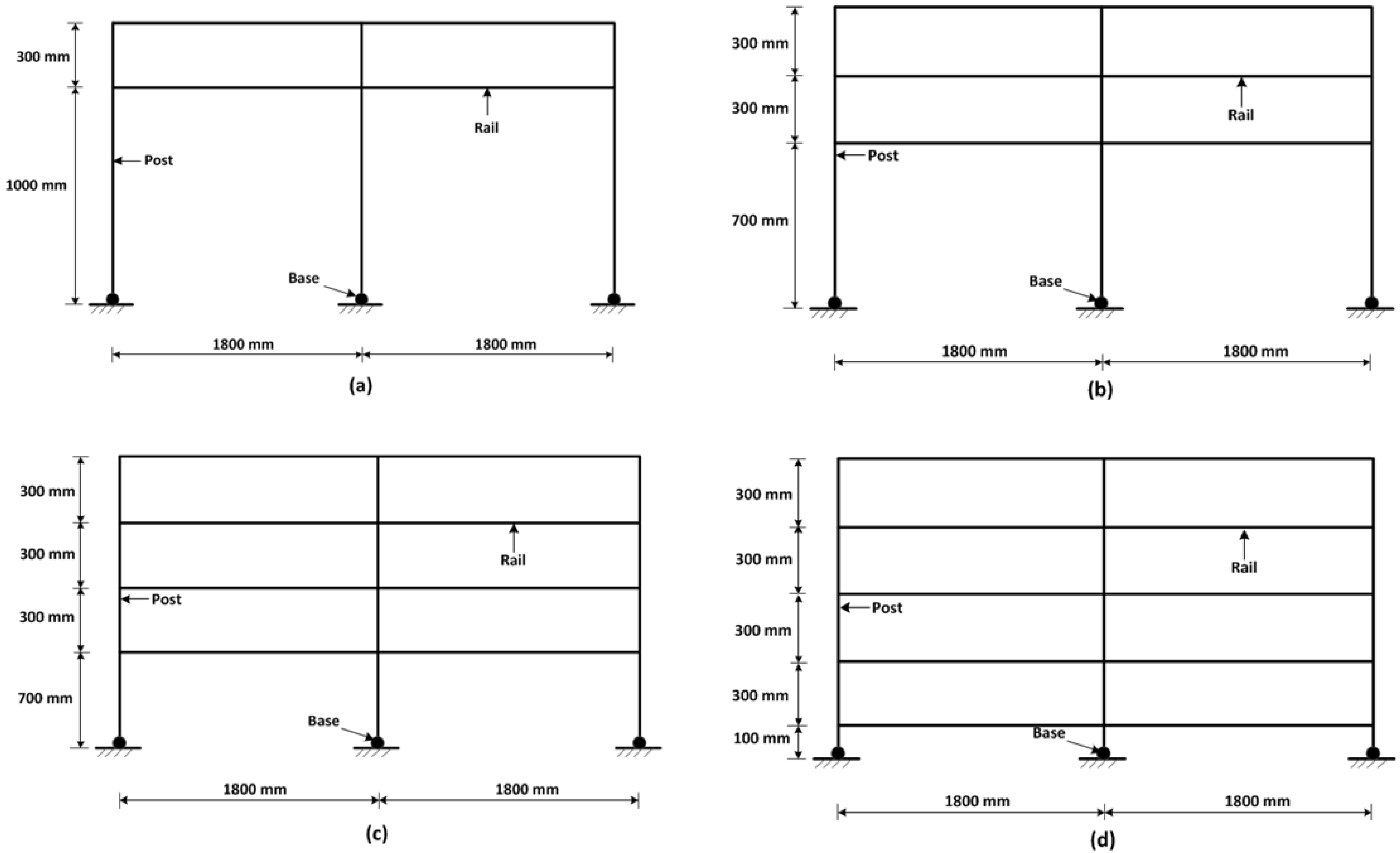

Figure 24: Details of the geometric layout with three posts and: (a) two rails (b) three rails (c) four rails and (d) five rails [not drawn to scale]

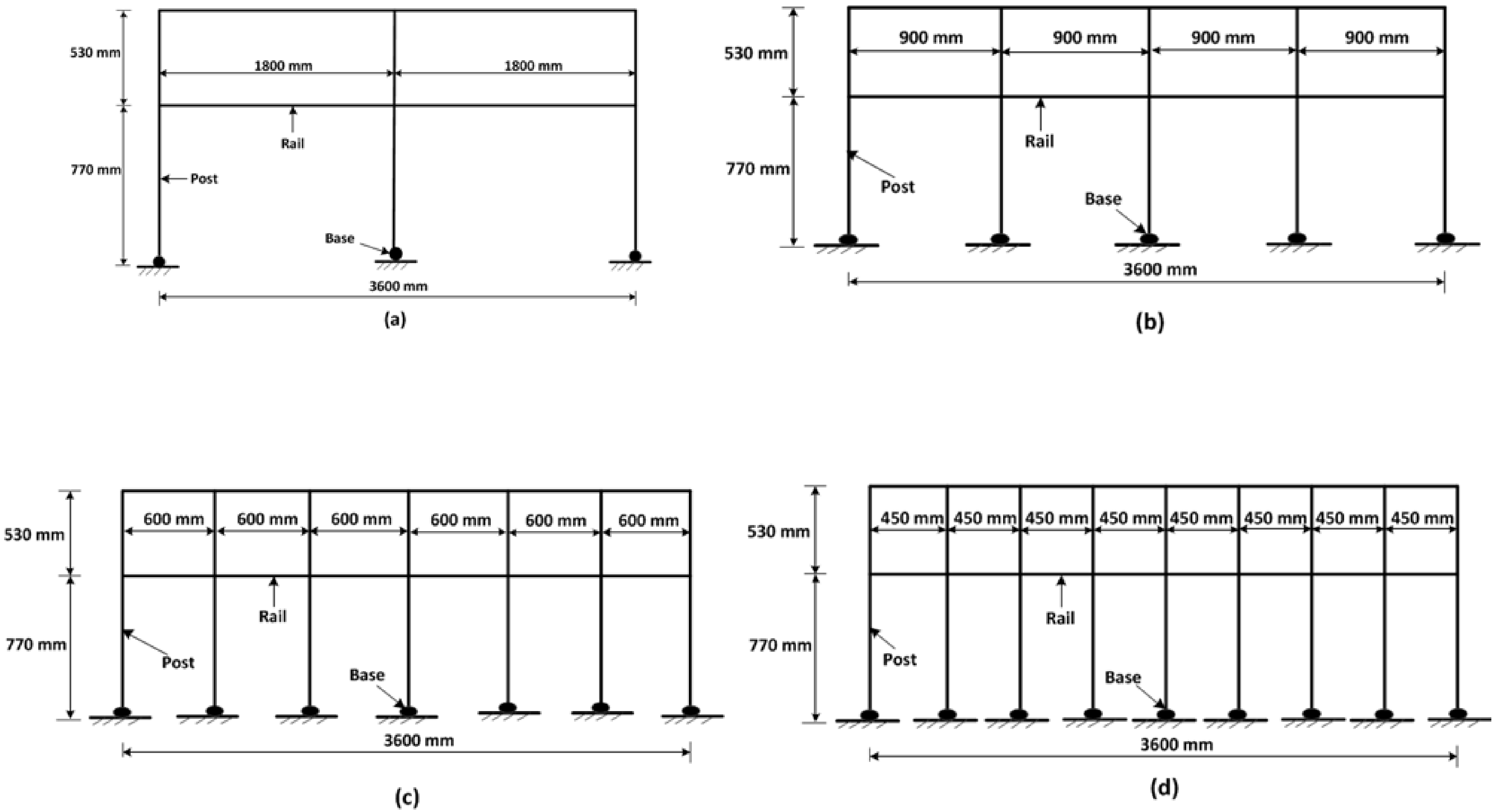

Figure 25: Details of the geometric layout with two rails and (a) three posts (b) five posts (c) seven posts (d) nine posts [not drawn to scale]

Figure 26 shows a plot of the maximum deflection against the number of the rails (2 – 5) based on an applied load of 1400 N at the top of the centre post. The result shows a gradual but insignificant reduction (approximately 6 %) in the maximum deflection from 78 to 73.6 mm, when the number of rails was increased from 2 – 5 rails. On the other hand, Figure 27 shows a plot of the maximum deflection against the number of posts (3 – 9); the result shows that an increase in the number of the posts led to a significant reduction in the maximum deflection.

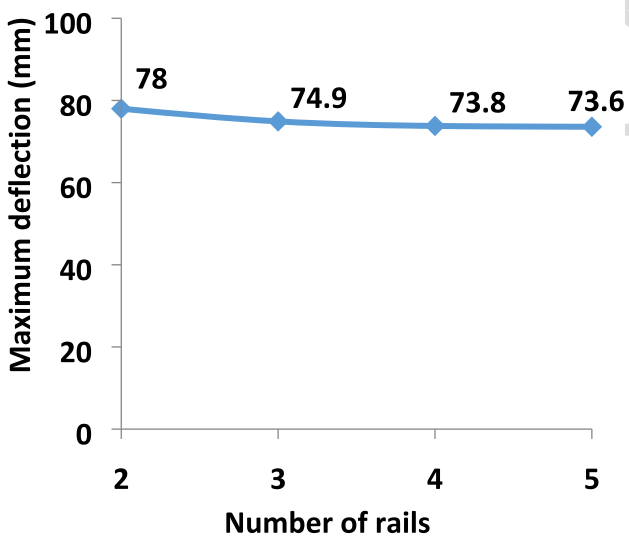

Figure 26: A plot of the maximum deflection against the number of the rails for an applied load of 1400 N at the top of the centre post

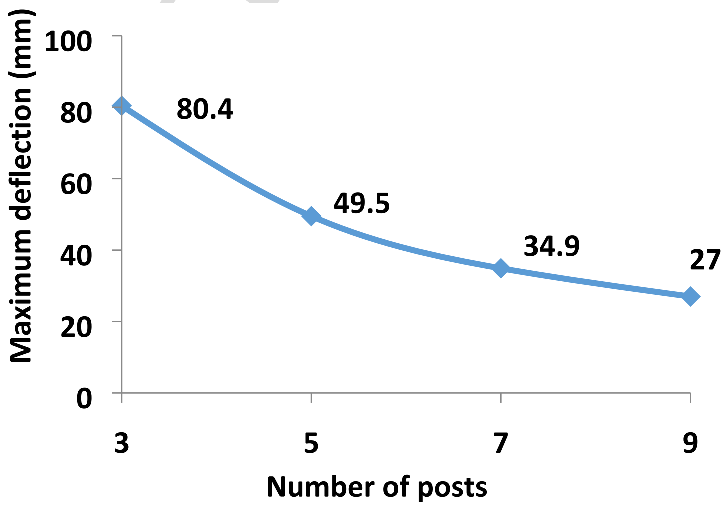

Figure 27: A plot of the maximum deflection against the number of the posts for an applied load of 1400 N at the top of the centre post

An increase in the number of the waste carpet structural composite posts from 3 to 9 posts led to a 66 % reduction in the maximum deflection, i.e. from 80.4 to 27 mm. It is evident that additional posts resulted in a greater reduction in the maximum deflection compared to an increase in the number of the rails.

Furthermore, based on the maximum deflection of 27 mm at an applied load of 1400 N (at the top of the centre post), the transverse stiffness for the geometric layouts with 9 posts (see Figure 25d) was 51.9 N/mm which is marginally greater than that of the two-bay timber fence of 50.7 N/mm (Sotayo et al., 2016). On the other hand, the transverse stiffnesses for the geometric layouts with 3, 5 and 7 posts were 17.4, 28.3 and 40.1 N/mm, respectively. These latter stiffnesses are lower than that of the timber fence, but are greater than that of the PVC fence (see Figure 21).

5.3. Optimisation of the Cross-Sections of the Waste Carpet Structural Composite Posts in the Geometric Layouts with 3, 5 and 7 Posts

Additional structural optimisations were carried out by increasing the depth of the posts by a factor of 2 (i.e. 71 to 142 mm) in increments of 5 mm for the geometric layouts with 3, 5 and 7 posts. The aim was to achieve a maximum transverse deflection similar to that of the timber fence, which was 27.6 mm and corresponds to a relative transverse stiffness of 50.7 N/mm. It should, therefore, be appreciated that there was no need to optimise the cross-section of the posts in the geometric layout with 9 posts (see Figure 25d), as it had a relative transverse stiffness of 51.9 N/mm (marginally greater than that of the timber fence). Figure 28 shows a plot of the maximum deflection against the depth of the posts for the geometric layouts with 3, 5 and 7 posts.

It should be noted that these maximum deflections are based on an applied load of 1400 N at the top of the centre post. The plots in Figure 28 all show a gradual reduction in the maximum deflection towards an asymptotic value. Increasing the depths of the posts by a factor of 2 (i.e. 71 to 142 mm) resulted in maximum deflections of 19.5, 14.4 and 10.3 mm for the geometric layouts with 3, 5 and 7 posts, respectively. These deflections also correspond to relative transverse stiffnesses of 71.8, 97.2 and 135.9 N/mm for the geometric layouts with

3, 5 and 7 posts, respectively. These aforementioned transverse stiffnesses are significantly greater than that of the timber fence, and produce a significant increase in the total mass of the posts and rails. In view of this, further structural analyses were carried out to examine the maximum deflections and transverse stiffnesses for each depth increment. The analyses show that a 69 % increase in the depth of the waste carpet structural composite posts for the geometric layout with 3 posts (shown in Figure 25a) resulted in a maximum deflection of 26.6 mm and corresponds to a transverse stiffness of 52.6 N/mm. Therefore, a width of 122 mm and a depth of 120 mm of the rectangular cross-section posts (compared to 122 mm by 71 mm) gives a relative transverse stiffness of 52.6 N/mm, which is slightly greater than that of the timber fence (50.7 N/mm).

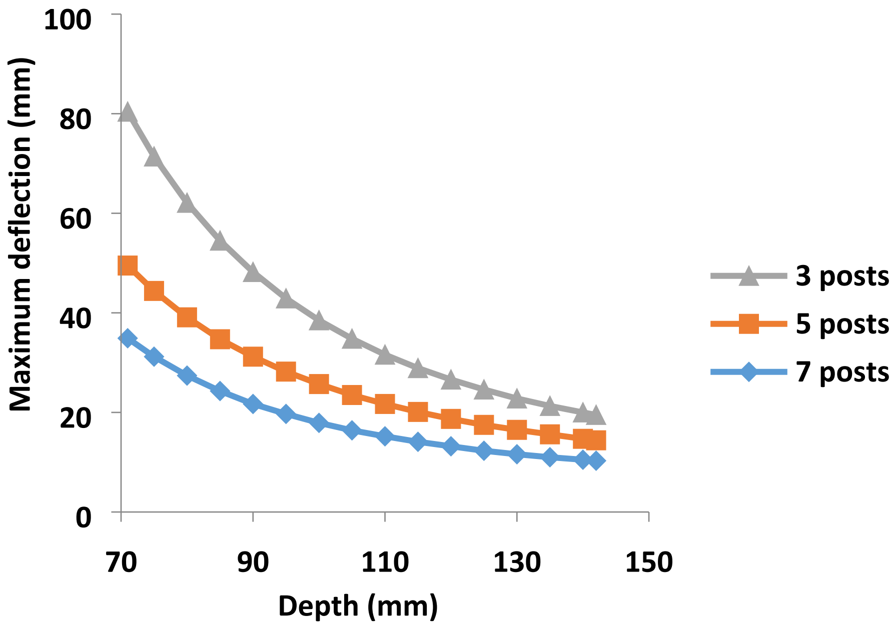

Figure 28: A plot of the maximum deflection against the depths of the posts for the geometric layouts with 3, 5 and 7 posts

Furthermore, a 41 % and 13 % increase in the depth of the waste carpet structural composite posts for the geometric layouts with 5 and 7 posts, (shown in Figure 25b and c) respectively, also resulted to transverse stiffnesses marginally greater than that of the timber fence. Therefore, for the geometric layout with 5 posts (Figure 25b), the rectangular cross-section dimensions of the posts may be 122 mm (width) by 100 mm (depth) without any changes to the cross-sections of the rails given in Table 6. Similarly, for the geometric layout with 7 posts (Figure 25c), the depths of the posts may be increased to 80 mm, to give a transverse stiffness approximately equal to that of the two-bay timber fence, whilst the width of the posts and cross-section dimensions of the rails remain the same as those given in Table 6.

6. Conclusion

Novel structural composites have been fabricated from carpet waste as an alternative waste management/recycling option to replace the landfill and incineration options. The benefits of this approach also include the replacement of timber and PVC posts and rails in fencing and other structural applications.

The manufacturing process of the waste carpet structural composites reported in this paper involved shredding, granulation and extrusion of strips of carpet waste, before being moulded with no second phase polymer addition and no mechanical separation of carpet fibres, which may have been costly and energy intensive. It was also demonstrated that the manufacturing process can be used for carpet waste with synthetic/man-made (i.e. polypropylene, nylon, PET) and/or natural (i.e. wool) face fibres, and therefore, offers the potential to recycle a large amount of carpet waste.

The experimental test setup, instrumentation and analysis techniques to determine the carpet composite's mechanical properties have been described, and the results have been analysed and discussed. The overall average elastic flexural modulus and strength were 2.6 GPa and 29.8 MPa, respectively. In addition, the uniaxial tensile tests carried out on flat specimens of the waste carpet structural composite material showed that the average elastic tensile modulus was 2.7 GPa, and the average tensile strength was 14.5 MPa. These experimental test results gave an understanding of some fundamental mechanical properties of the novel waste carpet structural composites. DIC combined with SEM images served to show that the failure modes may be attributed to the presence of voids, impurities and dirt particles in the raw material (waste carpet), as well as the type and source of carpet waste used.

As fencing structures are typically loaded to produce transverse bending under service loading, the flexural moduli of the post/rail components are important for evaluating their load-deformation responses. In view of this, the average flexural moduli for the waste carpet structural composite (2.6 GPa) and PVC (2.7 GPa) are reasonably close. On the other hand, the overall average flexural modulus for the waste carpet structural composite was only about a quarter of that of timber. Therefore, this paper investigated the use of novel waste carpet structural composites as the posts/rails of a fencing structure and compared them to similar timber and PVC fences using FE modelling and analysis. Prior to optimisation, the relative transverse stiffness of the two-bay waste carpet structural composite post and rail fence was 17.4 N/mm, which is 23 % greater than that of the PVC fence, and about 66 % lower than that of a similar timber fence. However, the optimisation processes demonstrated that additional posts and rails could be used to increase the overall transverse stiffness of the waste carpet structural composite fence. In particular, geometric optimisations of the cross-sections of the posts and/or increasing the number of the posts led to a greater increase in the relative transverse stiffness of the fencing structure compared to similar optimisations of the rails. It has been shown that a 69 % increase in the depth (from 71 to 120 mm) of the waste carpet structural composite posts resulted in a transverse stiffness similar to that of a similar timber fence.

Finally, the structural analyses and experimental testing reported herein have shown that changes to the cross-sections of the waste carpet structural composite posts/rails and their layout confirm the potential of recycled carpet waste composites as alternatives to common structural materials (i.e. timber and PVC) for fencing structures. Furthermore, the investigation also provides evidence in support of a novel remediation option for carpet waste with potentially significant economic and environmental benefits.

Acknowledgements

The authors wish to record their appreciation to the Centre for Global Eco-Innovation and the Engineering Department of Lancaster University for supporting their research. The Centre for Global Eco-Innovation is part-financed by the European Regional Development Fund (Grant no. X02646PR). In addition, thanks to Richard Wilbraham and Mohammed Milad for their assistance with the Scanning Electron Microscopy (SEM) analysis and Digital Image Correlation (DIC) operation, respectively.

References

BIRD, L. 2014. *Carpet Recycling UK Conference* [Online]. Carpet Recycling UK. Available: http://www.carpetrecyclinguk.com/downloads/27_percent_landfil_diversion_how_the_UK_exceeded_its_targets_two_years_early_Laurance_Bird_and_Jane_Gardner_Carpet_Recycling_UK.pdf [Accessed 26 July 2014].

CARPET RECYCLING UK. 2010. *Carpet Recycling and Government Policy* [Online]. Available: http://www.carpetrecyclinguk.com/downloads/Carpet_Recycling_and_Government_Policy_Jan%202010.pdf [Accessed 5 May 2014].

DEPARTMENT FOR ENVIRONMENT FOOD AND RURAL AFFAIRS. 2011. *Applying the Waste Hierarchy: evidence summary* [Online]. Available: https://www.gov.uk/government/uploads/system/uploads/attachment_data/file/69404/pb13529-waste-hierarchy-summary.pdf [Accessed 1 June 2014].

EUROPEAN UNION. 2010. *Being wise with waste: the EU's approach to waste management* [Online]. Available: http://ec.europa.eu/environment/waste/pdf/WASTE%20BROCHURE.pdf [Accessed 25 January 2014].

GARDNER, J. 2016. *Recycle your carpets, save on disposal costs, gain green credentials* [Online]. Available: http://www.carpetrecyclinguk.com/downloads/Recycle_your_carpets_save_on_disposal_costs_gain_green_credentials_Jane_Gardner_Carpet_Recycling_UK_20_09.pdf [Accessed 17 February 2017].

GOWAYED, Y. A., VAIDYANATHAN, R. & EL-HALWAGI, M. 1995. Synthesis of composite materials from waste fabrics and plastics. *Journal of Elastomers and Plastics,* 27**,** 79-90.

HELMS, M. M. & HERVANI, A. A. 2006. Reverse logistics for recycling: challenges facing the carpet industry. *Greening the supply chain.* Springer London.

IMETRUM. Available: http://www.imetrum.com/ [Accessed 25 April 2016].

JAIN, A., PANDEY, G., SINGH, A. K., RAJAGOPALAN, V., VAIDYANATHAN, R. & SINGH, R. P. 2012. Fabrication of structural composites from waste carpet. *Advances in Polymer Technology,* 31**,** 380-389.

MIHUT, C., CAPTAIN, D. K., GADALA-MARIA, F. & AMIRIDIS, M. D. 2001. Review: Recycling of nylon from carpet waste. *Polymer Engineering and Science,* 41**,** 1457-1470.

MIRAFTAB, M. & MIRZABABAEI, M. Carpet waste utilisation, an awakening realisation: a review. 2nd International Symposium on Fiber Recycling 11-12 May 2009 Atlanta, Georgia.

PALENIK, S. 1999. Microscopical Examination of Fibres. *In:* ROBERTSON, J. & GRIEVE, M. (eds.) *Forensic Examination of Fibres.* 2nd ed. London: Taylor and Francis.

SINGH, N., HUI, D., SINGH, R., AHUJA, I. P. S., FEO, L. & FRATERNALI, F. 2016. Recycling of plastic solid waste: A state of art review and future applications. *Composites Part B Engineering*.

SOTAYO, A., GREEN, S. & TURVEY, G. 2015. Carpet recycling: A review of recycled carpets for structural composites. *Environmental Technology & Innovation*.

SOTAYO, A., GREEN, S. & TURVEY, G. 2016. Experimental and Finite Element (FE) modelling of timber fencing for benchmarking novel composite fencing. *Composite Structures,* 158**,** 44-55.

SOTAYO, A., GREEN, S. & TURVEY, G. 2017. Experimental Investigation and Finite Element (FE) Analysis of the Load-Deformation Response of PVC Fencing Structures. Lancaster University.

THE CARPET AND RUG INSTITUTE. 2003. *THE CARPET PRIMER* [Online]. Available: http://www.carpet-rug.org/Documents/Publications/029_The_Carpet_Primer.aspx [Accessed 5 April 2014].

THERMO SCIENTIFIC. 2010. *Thermo Scientific Microphazir PC Handheld Carpet Fiber Identification* [Online]. Available: http://www.thermoscientific.com/content/dam/tfs/ATG/CAD/CAD%20Documents/Product%20Manuals%20&%20Specifications/Portable%20Analyzers%20for%20Material%20ID/Handheld%20NIR/microPHAZIRPC-Carpet-analyzer.pdf [Accessed 2nd September 2015].

UK GOVERNMENT. 2016. *Landfill Tax: increase in rates* [Online]. Available: https://www.gov.uk/government/publications/landfill-tax-increase-in-rates/landfill-tax-increase-in-rates [Accessed 17 February 2017].

VAIDYANATHAN, R., SINGH, R. P. & LEY, T. 2013. Recycled Carpet Materials for Infrastructure Applications. Oklahoma: Oklahoma Transportation Centre.

WAGHORN, H. & SAPSFORD, P. 2017. The Replacement of Wood or Concrete in Construction Projects: An Industrial Case Study Demonstrating the Benefits of Intrusion Moulded Waste Plastic. *In:* DASTBAZ, M., GORSE, C. & MONCASTER, A. (eds.) *Building Information Modelling, Building Performance, Design and Smart Construction.* Springer International Publishing.

ZHANG, Y., MUZZY, J. D. & KUMAR, S. 1999. Recycling carpet waste by injection and compression molding. *Polymer-Plastics Technology and Engineering,* 38**,** 485-498.

Highlights

- Novel structural composite materials were fabricated from carpet waste.
- Experimental characterisation tests were carried out on waste carpet composites.
- FE analysis was used to simulate the response of a carpet composite fence.
- Design optimisations were carried out on the carpet composite fence.
- Carpet composite offers potential as an alternative to timber and PVC posts/rails.